Annular α-Synuclein Protofibrils Are Produced When Spherical Protofibrils Are Incubated in Solution or Bound to Brain-Derived Membranes†

Tomas T. Ding, Seung-Jae Lee,‡ Jean-Christophe Rochet, and Peter T. Lansbury, Jr.*

Center for Neurologic Diseases, Brigham and Women's Hospital, and Department of Neurology, Harvard Medical School, 65 Landsdowne Street, Cambridge, Massachusetts 02139

Received February 18, 2002; Revised Manuscript Received April 25, 2002

ABSTRACT: The Parkinson's disease *substantia nigra* is characterized by the loss of dopaminergic neurons and the presence of cytoplasmic fibrillar Lewy bodies in surviving neurons. The major fibrillar protein of Lewy bodies is α-synuclein. Two point mutations in the α-synuclein gene are associated with autosomal-dominant Parkinson's disease (FPD). Studies of the in vitro fibrillization behavior of the mutant proteins suggest that fibril precursors, or α-synuclein protofibrils, rather than the fibrils, may be pathogenic. Atomic force microscopy (AFM) revealed two distinct forms of protofibrillar α-synuclein: rapidly formed spherical protofibrils and annular protofibrils, which were produced on prolonged incubation of spheres. The spherical protofibrils bound to brain-derived membrane fractions much more tightly than did monomeric or fibrillar α-synuclein, and membrane-associated annular protofibrils were observed. The structural features of α-synuclein annular protofibrils are reminiscent of bacterial pore-forming toxins and are consistent with their porelike activity in vitro. Thus, abnormal membrane permeabilization may be a pathogenic mechanism in PD.

The ordered fibrillization of highly expressed but typically soluble proteins is a characteristic of many neurodegenerative diseases (*1*). The possibility that fibrillization of the abundant neuronal protein α-synuclein (*2*) may initiate Parkinson's disease (PD)[1] pathogenesis (*3*−*5*) is suggested by the following: (1) in terms of pathological evidence, α-synuclein is the major component of the fibrils of Lewy bodies, the neuronal inclusions that are characteristic of the degenerating *substantia nigra* (*6*, *7*), and (2) in terms of genetic evidence, two point mutations in the α-synuclein gene (A53T and A30P) are associated with rare autosomal-dominant forms of PD (*8*−*10*). Accordingly, animal models of PD have been generated on the basis of the proposal that α-synuclein fibrillization causes neurodegeneration. Expression of wild-type (WT) or mutant (A30P and A53T) human α-synuclein in transgenic *Drosophila* (which lack endogenous α-synuclein) leads to fibrillar, Lewy body-like inclusions, dopaminergic cell loss, and age-related motor dysfunction (*11*). Coexpression of HSP70 slows the loss of dopaminergic neurons, but does not significantly decrease the number of fibrillar inclusions, suggesting that fibrils do not cause cell death (*12*). In contrast to *Drosophila*, transgenic mice that express human WT α-synuclein produce nonfibrillar inclusions. However, like *Drosophila*, the transgenic mice develop Parkinsonian phenotypes, motor deficits and loss of dopaminergic termini (*13*), consistent with the notion that a prefibrillar form of α-synuclein, rather than the fibril itself, may be pathogenic (*5*, *14*, *15*). Crossing the α-synuclein trangenic mice with the *β*-synuclein-expressing line produces bigenic mice in which all three phenotypes are virtually eliminated (*16*).

The "toxic protofibril" hypothesis is also supported by in vitro studies of α-synuclein fibrillization (*4*, *5*, *17*, *18*). Although α-synuclein lacks stable structure in dilute solution (*19*−*21*), it produces *β*-sheet rich oligomers, or protofibrils, when concentrated (*20*, *22*). Protofibrils are heterogeneous and, by definition, transient; they appear to be directly incorporated into amyloid fibrils (*23*, *24*). Both PD-associated mutations (A53T and A30P) affect the rate of population of the protofibrillar intermediates, as well as their persistence (*17*, *25*). However, A30P populates the fibrillar state more slowly than WT, suggesting that protofibrils, rather than fibrils, may be pathogenic (*17*). Studies of the protofibrillar species demonstrated the existence of spherical and annular morphologies (*17*, *22*). The studies reported here were undertaken to characterize these species in more detail and to elucidate their interaction with crude brain-derived vesicular material.

EXPERIMENTAL PROCEDURES

Preparation of α-Synuclein Protofibrils. Recombinant α-synucleins (WT, A53T, and A30P) were produced in *Escherichia coli* and purified according to published methods (*27*). Spherical protofibrils were prepared according to two

† This work was supported by the National Institutes on Aging (Grant AG14366), the National Institutes of Neurological Disorders and Stroke (Morris K. Udall Parkinson's Disease Research Center of Excellence Grant NS38375), the James K. Warsaw Foundation to Cure Parkinson's Disease, and the Kinetics Foundation. J.-C.R. is grateful to the Human Frontier Science Program and the Alberta Heritage Foundation for Medical Research.

* To whom correspondence should be addressed. E-mail: plansbury@rics.bwh.harvard.edu.

‡ Current address: The Parkinson's Institute, Sunnyvale, CA.

[1] Abbreviations: AFM, atomic force microscopy; *β*-PFTs, *β*-sheet pore-forming toxins; FPD, familial Parkinson's disease; HSP, heat shock protein; IAPP, islet amyloid polypeptide; PD, Parkinson's disease; SD, standard deviation; WT, wild-type.

10.1021/bi020139h CCC: $22.00 © 2002 American Chemical Society
Published on Web 07/20/2002

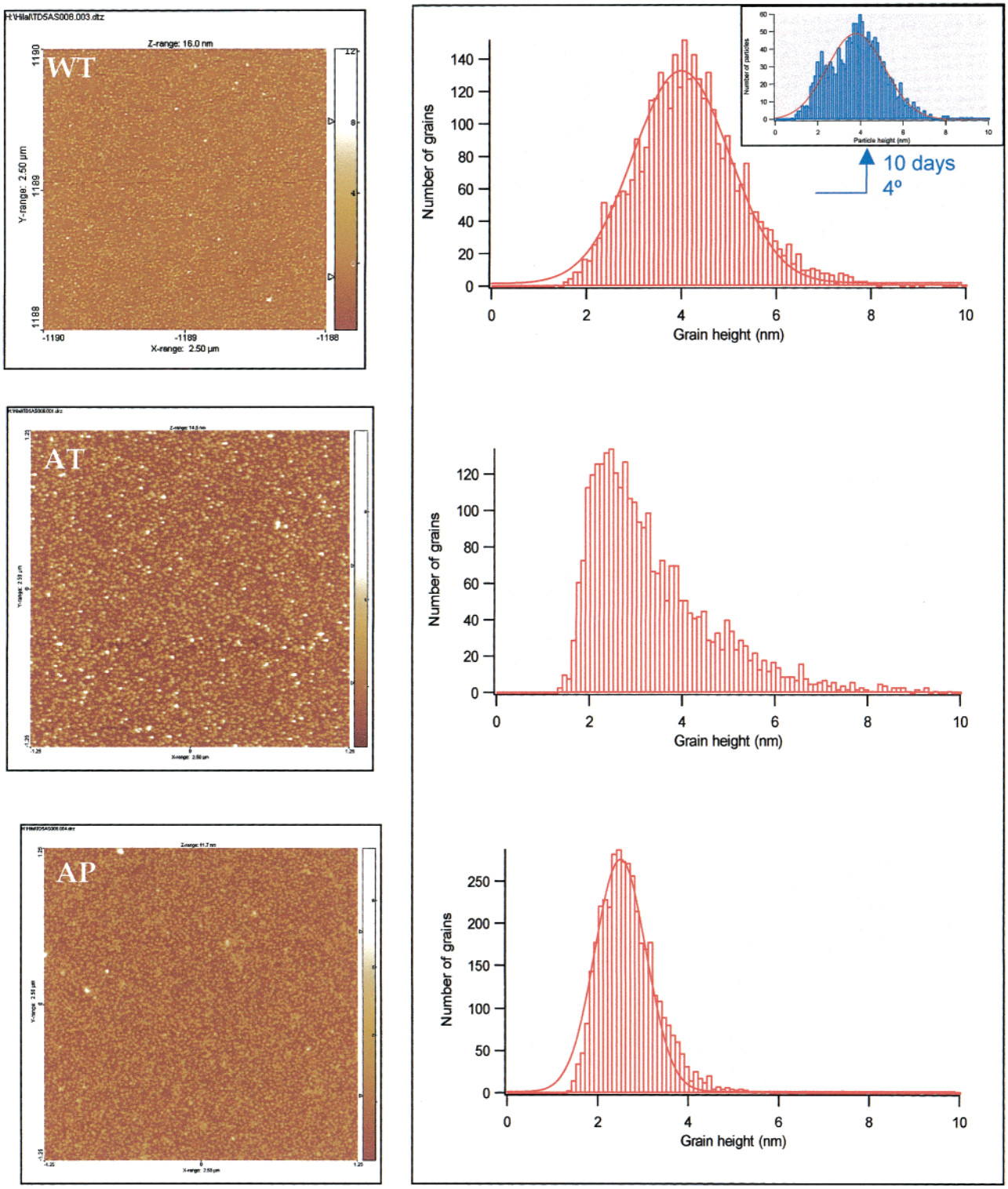

FIGURE 1: Spherical protofibrils of WT, A53T, and A30P α-synuclein. The panels on the left show typical AFM images (2.5 μm scan size) of spherical protofibrils (stored in buffer at 4 °C). The right panels show height distribution histograms for the corresponding images in the left column. WT: arithmetic mean of 4.2 nm, SD of 1.2 nm, gauss fit mean of 4.0 nm, gauss fit variance of 1.4 nm, $n = 3503$. AT: arithmetic mean of 3.4 nm, SD of 1.4 nm, $n = 2993$. AP: arithmetic mean of 2.7 nm, SD of 0.7 nm, gauss fit mean of 2.5 nm, gauss fit variance of 0.8 nm, $n = 4048$. The WT spherical protofibrils convert, over time, to spheres with dimensions similar to those of A30P (see the inset of the top right panel).

protocols. In method A, protofibrillar material was formed slowly from monomer. The protofibrillar (void volume) fraction from an incubation of filtered, monomeric α-synuclein as described in ref *20* was utilized. This method was impractical for producing large amounts of protofibrillar material. In method B, a much greater amount of protofibrillar material was formed rapidly during isolation and lyophilization. A concentrated solution of α-synuclein (1−2 mM) was prepared by dissolving the lyophilized protein in 50−100 μL of phosphate-buffered saline (PBS) at 4 °C. The solution was filtered by centrifugation (3000*g*) through a 0.22 μm nylon spin filter (Costar). For both methods A and B,

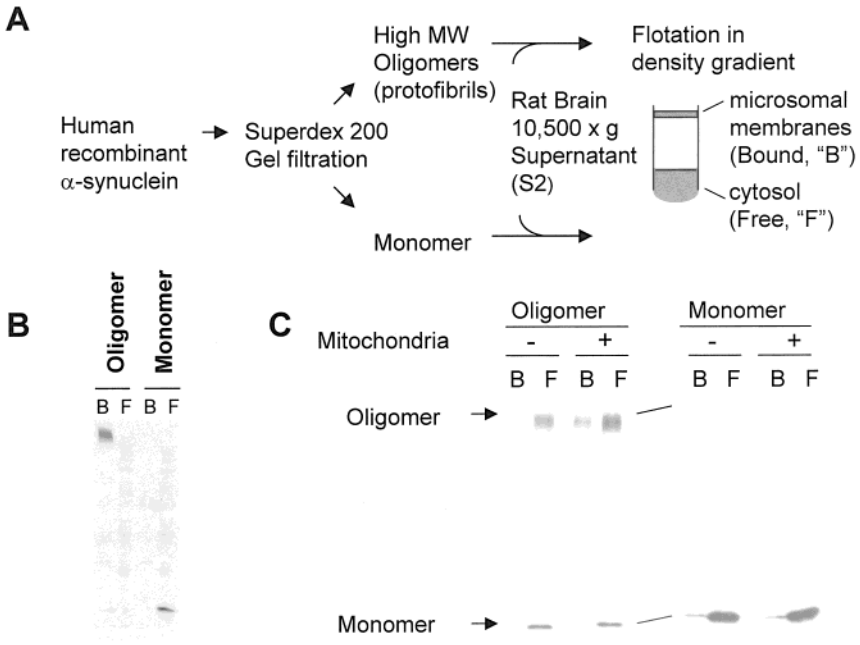

FIGURE 2: Difference in binding of α-synuclein monomer and protofibrils to brain-derived membranes. (A) Schematic representation of the procedure used. Purified protofibrils or monomer was incubated with BDV membranes (B) or mitochondria (C). Vesicle-associated proteins (B for bound) were separated from free proteins (F for free) by density gradient centrifugation and analyzed by SDS−PAGE (protofibrils were characterized by a high-MW, LB509-positive band). (B) Protofibrillar and monomeric α-synuclein fractions were incubated with brain-derived microsomal vesicles. Protofibrils bound to brain vesicles much more avidly than did monomer (LB509 does not recognize endogenous brain microsomal α-synuclein). (C) Binding of protofibrillar α-synuclein to brain mitochondria. Protofibrillar (oligomeric, lanes 1−4) or monomeric (lanes 5−8) α-synuclein was incubated (25 °C for 1 h) in the presence (lanes 3, 4, 7, and 8) or absence (lanes 1, 2, 5, and 6) of isolated rat brain mitochondria. Only the protofibrillar protein showed affinity for mitochondria.

the filtered protein solution was eluted from a Superdex 200 gel-filtration column (1.0 cm in diameter and 30 cm in height) in PBS at a flow rate of 0.5 mL/min, and the eluate was monitored at 215 nm. Material included in the void volume (defined as the elution volume of Blue Dextran 2000) contained oligomeric α-synuclein and was stored at 4 °C prior to AFM analysis. All incubations were carried out in the absence of agitation or stirring.

Fractionation of Rat Brain Tissue. The fractionation of vesicles by differential centrifugation was carried out at 4 °C. Two adult rat cerebrums were Dounce-homogenized in 8 mL of vesicle binding buffer (VBB) [25 mM HEPES (pH 7.2), 200 mM sucrose, 50 mM KCl, and 1 mM $MgCl_2$] supplemented with protease inhibitor cocktail (Sigma). After centrifugation (10 min at 1100*g*), the supernatant (S1, pellet is P1) was subjected to centrifugation (15 min at 10500*g*) and the resultant supernatant (S2) used for membrane binding experiments. Mitochondria were isolated from rat brain (*28*). The forebrain was washed and homogenized in isolation buffer [10 mM Tris (pH 7.4), 0.32 M sucrose, and 1 mM EDTA] using a motor-assisted Potter-Elvehjem homogenizer with a Teflon pestle. The homogenate was subjected to centrifugation (1330*g* for 3 min), and the resultant supernatant was subjected to further centrifugation at a higher speed (21200*g* for 10 min). The resulting pellet was resuspended [15% (v/v) Percoll] and prepared in isolation buffer (10 mL/g of original homogenate). The crude mitochondrial suspension in 15% Percoll was layered onto a discontinuous density gradient consisting of 23% Percoll layered above 40% Percoll, and subjected to centrifugation (30700*g* for 10 min). The pure mitochondrial band was visible near the interface of the two lower Percoll layers. After 1:4 dilution with isolation buffer, mitochondria were subjected to centrifugation (16700*g* for 10 min) and washed with isolation buffer (3 mL) containing fatty acid-free bovine serum albumin (5 mg). The washed mitochondria were reisolated by centrifugation (6900*g* for 10 min). The mitochondrial pellet was resuspended in 0.3 mL of isolation buffer.

Membrane Binding Assay. The S2 microsomal fraction (0.4 mL) was incubated with 0.5 μg of protofibrillar or monomeric α-synuclein freshly purified by gel filtration for 2 h at 25 °C. The membrane-bound and free α-synuclein fractions were separated by membrane flotation (*29*). The binding reaction mixture was mixed with 0.42 mL of 60% iodixanol gradient medium (Life Technologies, Inc.), and overlaid with 2.5 mL of 25% iodixanol and 0.1 mL of 5% iodixanol in VBB. The step gradient was centrifuged for 2 h at 200000*g* in an SW55.1 rotor (Beckman) at 4 °C. Microsomal vesicles, along with associated proteins, were collected in the interface between the 5 and 25% iodixanol layers, and the free, unbound proteins were collected from the bottom of the tube. For mitochondrial binding, purified mitochondria (or isolation buffer alone as a control) were incubated with 0.5 μg of α-synuclein protofibril or monomer for 1 h at 25 °C. Bound and free α-synuclein fractions were separated (centrifugation at 10000*g* for 3 min). The mitochondrial pellet was washed with isolation buffer twice followed by centrifugation. Western blotting (*30*) utilized LB509 or H3C as a primary antibody. LB509 (Zymed Laboratories Inc., South San Francisco, CA) recognizes human α-synuclein, but not the rat or mouse homologue. Antibody H3C (a gift from D. Clayton, University of Illinois, Urbana, IL) recognizes both human and mouse α-synuclein.

Kinetic Analysis of Formation of Membrane-Binding Protofibrils. Lyophilized purified α-synuclein was reconstituted in PBS (pH 7.4) and 0.02% NaN_3 and filtered through

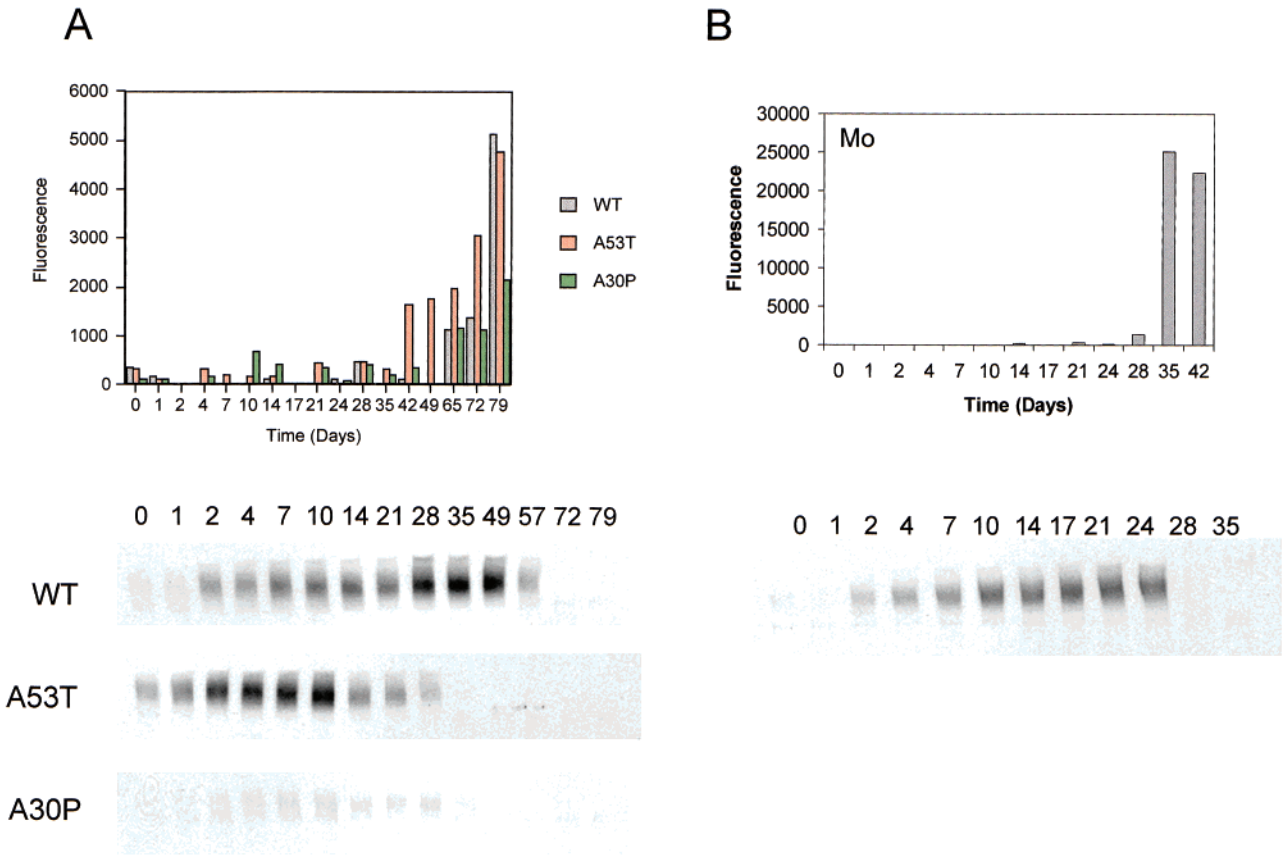

FIGURE 3: Membrane-binding form of α-synuclein which forms slowly and is consumed as fibrils appear. (A) Time course for the formation of amyloid fibrils (thioflavin T, top) and BDV-bound protofibrils (WT, A53T, and A30P) from prefiltered, monomeric α-synuclein (Western blotting with LB509). (B) Similar time course for the mouse protein, which fibrillizes more rapidly than all human variants in vitro (Western blotting with H3C) (*27*).

a Millipore Microcon 100K MWCO filter. The samples were dialyzed against PBS (pH 7.4) and 0.02% NaN_3 at 4 °C overnight to remove salt. The protein concentration was adjusted to 230 μM (quantitative amino acid analysis), and solutions were incubated at 37 °C without agitation. Aliquots were taken periodically for the membrane binding assay using the brain S2 fraction and the fibrillization assay (thioflavin T fluorescence) (*17*, *31*, *32*).

Atomic Force Microscopy. The incubations were mixed gently to suspend any aggregates; a 3−4 μL aliquot of the mixture was placed on freshly cleaved mica (Ted Pella, Redding, CA). The contents were allowed to adsorb for 1−2 min before the droplet was displaced with a 100 μL portion of Millipore-filtered water. Excess water was removed with a gentle stream of filtered, compressed trifluoroethane (Dust-Off Plus, Falcon Safety Products, Branchburg, NJ) (note that the sample is assumed to remain hydrated after this treatment). Images were obtained with a Nanoscope IIIa Multimode scanning probe workstation equipped with an E-scanner and operating in the tapping mode (Digital Instruments, Santa Barbara, CA), using etched silicon NanoProbes (model FESP, Digital Instruments). Scanning parameters varied with individual tips and samples. Some typical values were as follows: free oscillation amplitude, 500−900 mV; drive frequency, 70−80 kHz; setpoint, 400−800 mV; and scan rate, 1−1.49 Hz. The images were analyzed using the Nanoscope software and the Scanning Probe Image Processor (SPIP, Imagemetrology, Lyngby, Denmark).

Tapping Mode Atomic Force Microscopy of Brain-Derived Microsomal Membranes Adsorbed on Mica. AFM specimen preparation and imaging were carried out in air at ambient temperature. Samples containing brain-derived microsomal vesicles were mixed gently to suspend aggregates, and 5−10 μL aliquots of the mixtures were placed on freshly cleaved mica (Ted Pella), incubated for 60−90 s, and then washed with 100 μL of filtered deionized water. Droplets of water were removed with a gentle stream of filtered compressed trifluoroethane (Dust-Off Plus, Falcon Saftey Products). The samples were imaged *immediately*, using a Nanoscope IIIa Multimode scanning probe workstation equipped with an E-scanner (Digital Instruments) and etched silicon Nano-Probes (model FESP, Digital Instruments). Scanning parameters varied with individual tips and samples. Some typical values were as follows: free oscillation amplitude, 15−20 nm; drive frequency, 70−80 kHz; setpoint, 400−500 mV; and scan rate, 1−1.49 Hz. The images were analyzed using built-in applications of the Nanoscope software; Flatten (zero-order) and Plane fit (automatic, first-order) were applied to the images to correct for artificially generated bends and tilts of the image plane. Surface anatomy was analyzed in detail using the "section" application in the Nanoscope software.

RESULTS

Spherical Protofibrils Are Formed Rapidly and Subsequently Convert to a More Compact Spherical Species. α-Synuclein protofibrils were formed in vitro and characterized by atomic force microscopy (AFM) (*17*, *20*, *33*). The

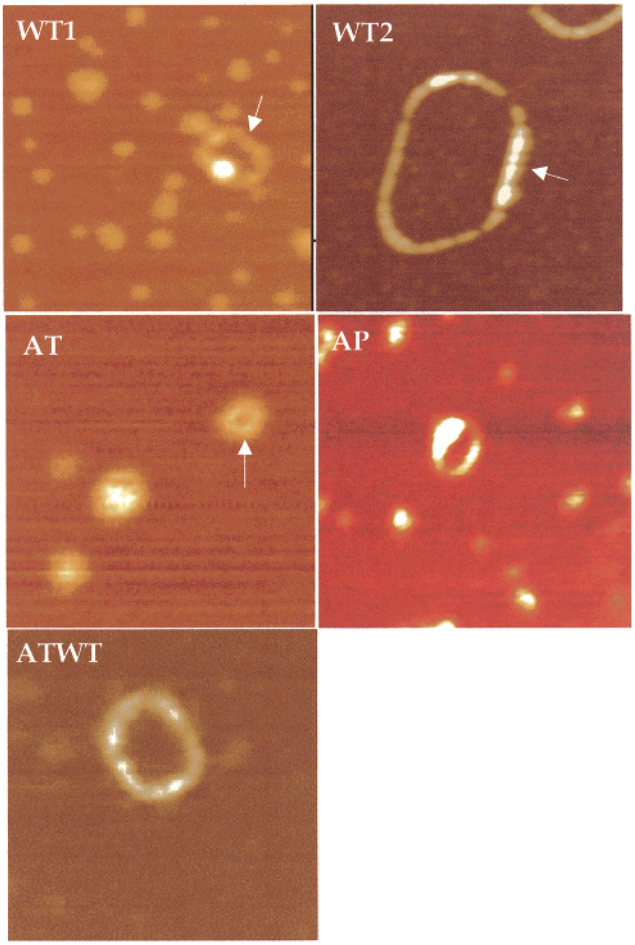

FIGURE 4: Typical annular protofibrils comprising WT, A53T, a 1:1 WT/A53T mixture, and A30P. Two types of WT annular structures were observed to form in solution, in the absence of membranes, WT1 (see arrow) and WT2. The WT1 structure is decorated by a spherical protofibril. AT shows A53T annular structures by AFM (see arrow). A WT/A53T annular structure is shown in ATWT. AFM image sizes are 250 nm for A30P, WT1, and ATWT, 500 nm for WT2, and 100 nm for AT. "WT2-like" annular protofibrils have not been observed in incubations containing A30P or A53T.

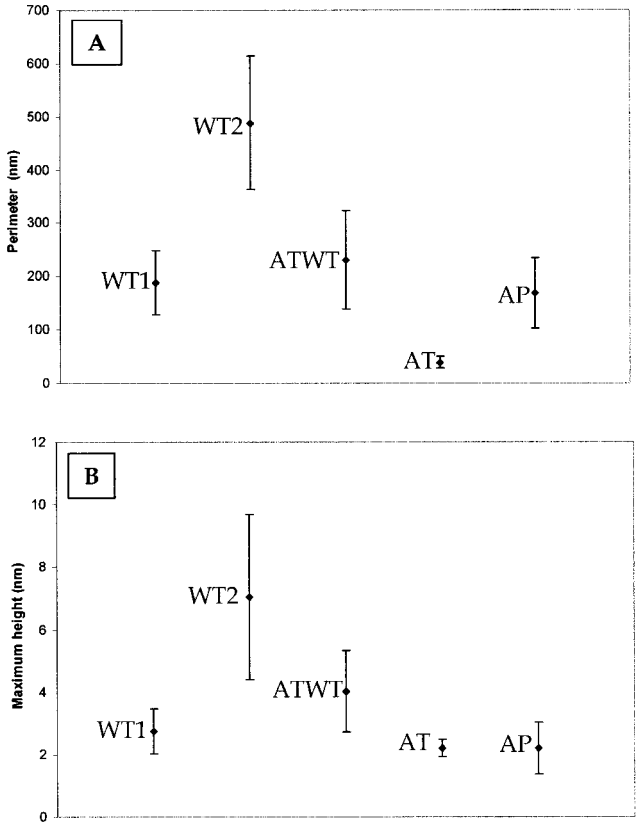

FIGURE 5: Characterization of annular protofibrils shown in Figure 4. (A) Average perimeters for the α-synuclein annular protofibrils shown in Figure 4. (B) Average maximum heights for α-synuclein annular protofibrils. Mean heights are not shown here. ATWT is significantly higher than WT1 ($p < 0.00001$, Student's t test), AT ($p = 0$, Student's t test), and AP ($p < 0.00001$, Student's t test). WT1 and AP annular protofibrils have the same perimeters and heights, while the variances of the perimeter distributions differ ($p < 0.005$, paired F test); see the text for details. The variance of the AP distrubution is also significantly different from the variance of the ATWT distribution ($p < 0.00001$, paired F test). The maximum height of α-synuclein amyloid fibrils is typically 9−10 nm (*20*). Error bars represent ±1 SD.

first-formed α-synuclein protofibrils appeared to be predominantly spherical[2] with heights varying between 2.5 and 4.2 nm (Figure 1) (*17*). It is important to note that since heights measured by AFM reflect sample compressibility, a "soft" object could appear to be shorter than a "hard" one (thus, the measured height is the lower limit of the true height). Both WT and A30P produced spherical protofibrils with a Gaussian distribution of heights, albeit of different absolute height values [mean heights, 4.2 nm for WT (Figure 1, top) and 2.7 nm for A30P (Figure 1, bottom)]. After incubation for an identical period of time, A53T produced a population of spheres that appeared to be a mixture of these two types, with predominantly A30P-like compact spheres (Figure 1, middle). Prolonged incubation of WT spheres (10 days at 4 °C) resulted in the appearance of a more compact population resembling A30P spheres (Figure 1, inset). After 13 days, the distribution had shifted further toward the more compact population (not shown), suggesting that the 2.7 nm spherical protofibrils are the "mature" form of the spherical protofibril. This height is similar to that of subsequently formed protofibrils (see below).

Spherical α-Synuclein Protofibrils Bind to Brain Microsomal Membranes and Mitochondria Much More Tightly Than Does α-Synuclein Monomer. The membrane binding ability of protofibrillar α-synuclein (spheres) was compared to that of the monomeric form using a crude sedimentation assay. Protofibrillar α-synuclein has a much greater affinity for synthetic vesicles than does the monomeric protein (*22*). Similarly, protofibrillar α-synuclein had a far greater affinity for a crude brain-derived membrane fraction than did the α-synuclein monomer (Figure 2B). A significant, but less pronounced, difference was seen with crude mitochondria (Figure 2C).

Membrane-Binding α-Synuclein Protofibrils Form Slowly and Disappear before Fibrils Are Detected. The generation of a membrane-binding subfraction of α-synuclein oligomers from monomeric α-synuclein was slow, requiring days to weeks. This species disappeared as fibrils appeared, although a time lag was observed between its disappearance and fibril appearance in the cases of A53T and A30P, but not the WT or mouse variants (Figure 3). Similarly, the *total* protofibril population grows and is converted to fibrils (*14*), but in this

[2] Chainlike protofibrils were observed on prolonged incubation of A30P (*27*).

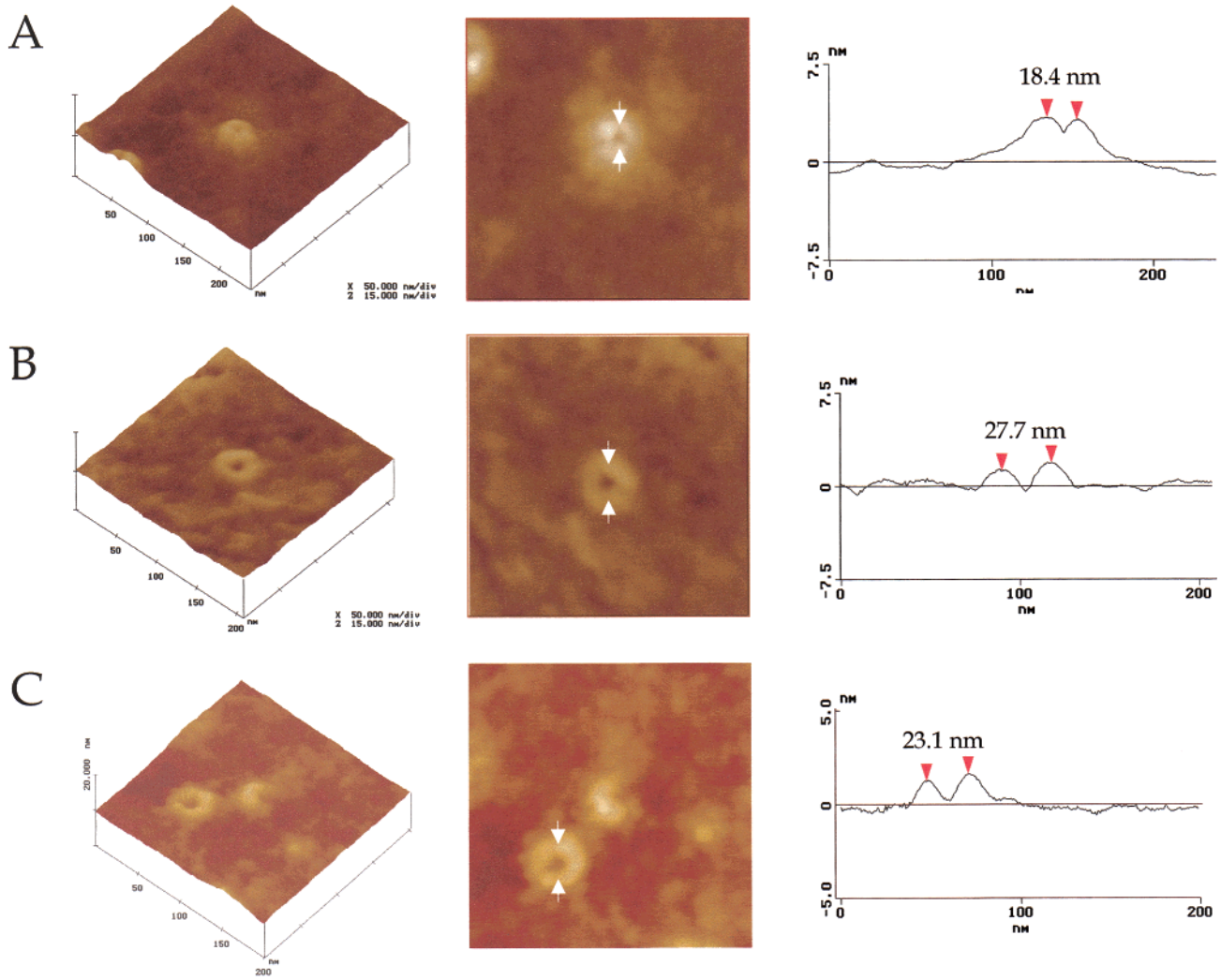

FIGURE 6: AFM images showing membrane-bound annular structures. Images (~200 nm^2, shown in two perspectives) of porelike structures that were obtained by incubating predominantly spherical α-synuclein protofibrils (WT in panels A and B and A53T in panel C) with brain-derived vesicles. Arrows on images show the points that determine the cross sections depicted at the right. Note the crescent structure in panel C.

case, protofibrils persisted until fibrils appeared, confirming that the membrane-binding subfraction does not necessarily behave like the typical protofibril. The rate of the formation and consumption of membrane-binding α-synuclein protofibrils was sensitive to the FPD mutations. A53T and A30P membrane-binding protofibrils were detected at day 1 (A53T) or day 2 (A30P) and peaked around 10 days. In contrast, WT membrane-binding protofibrils were first detected at 2 days and peaked around 49 days (Figure 3A). Interestingly, this trend did *not* directly correlate with the lag time for fibril formation; A53T fibrils were detected first (~42 days), followed by WT and A30P (~65 days). Furthermore, the *amount* of membrane-binding protofibrils (estimated from Western blots) formed during fibrillization appeared to be smaller in the case of A30P than that of either A53T or WT [mouse α-synuclein, which fibrillizes much more rapidly than any human variant (*14*), also rapidly populated a membrane-binding protofibrillar form (4 days)]. However, for PD pathogenesis, it is the amount of toxic protofibril, not the amount of total protofibril, that is critical. Protofibrillar A30P and A53T populations have a greater in vitro permeabilizing activity per mole of α-synuclein than WT (*26*).

Spherical α-Synuclein Protofibrils Convert to Annular Structures. Spherical α-synuclein protofibrils were incubated at 4 °C; aliquots were removed at regular time intervals, and AFM specimens were prepared by adsorption to mica. Annular protofibrils were produced from spherical protofibrils comprising WT, A53T, and A30P and a 1:1 WT/A53T mixture (Figure 4). No annular protofibrils were detected after incubation of monomeric α-synuclein under identical conditions. After 2 weeks at 4 °C, WT spherical protofibrils produced two types of annular structures, small (WT1, diameter range of 32−96 nm, Figures 4 and 5B) and large (WT2, diameter range of 100−180 nm, Figures 4 and 5B). WT1 could also be produced directly by incubation of WT spherical protofibrils at 37 °C. The ~3 nm height of the WT1 annular protofibrils was consistent with their comprising a ring of compact spherical protofibrils. The WT2 annular protofibrils were characterized by discrete ~7 nm height regions (see the arrowhead in Figure 4). These regions resembled the α-synuclein amyloid fibril and may represent short stretches of fibril-like morphology (*27*).

FPD-Linked Mutations Affect the Diameter of the Annular Protofibrils. When incubated under conditions similar to

those of WT (see above), A53T spherical protofibrils (produced by method B; see Experimental Procedures) converted to a relatively homogeneous population of small annular protofibrils (~10 nm in diameter, Figure 5A). Analysis of the *crude* A53T incubation product by electron microscopy revealed numerous annular protofibrils (H. Lashuel et al., manuscript submitted for publication). Spherical protofibrils produced from a 1:1 mixture of monomeric A53T and WT (by method A, see Experimental Procedures) were converted to a more heterogeneous population of predominantly larger annular structures (diameter range of 50−100 nm, some ~30 nm diameter structures were observed; Figures 4 and 5). The WT/A53T and WT annular protofibril populations differed significantly with respect to their mean height (data not shown, 1.3 nm for WT1 vs 2.7 nm for WT/A53T). Annular A30P protofibrils were also formed by incubating A30P spherical protofibrils (method B) at an elevated temperature (48 h at 37 °C, annular structures were not detected in 4 °C incubations). The A30P annular structures had a segmented, triangular appearance, different from the apparently flexible structures comprising WT (compare Figure 4, AP vs WT1). The dimensions of the A30P annular protofibrils (diameter of 55 nm and maximum height of 2.2 nm) were similar to those of WT1, but the A30P protofibril population was more homogeneous (perimeter *variances* were different; F test, $p < 0.005$). For all of the experiments described above, it is important to note that AFM allows the *selective* observation of only those species that adsorb onto the mica surface. Since AFM does not detect all species, an AFM image does not necessarily accurately reflect the distribution of species. Studies of α-synuclein protofibrils with electron microscopy indicate that some annular protofibrils may not be efficiently adsorbed (H. Lashuel et al., unpublished observations).

Incubation of Spherical α-Synuclein Protofibrils with Brain-Derived Membranes Produces Porelike Annular Protofibrils. Given the high affinity of the spherical protofibrils for brain-derived microsomal membranes (Figures 2 and 3), we sought to directly observe the membrane-bound species by AFM. Vesicular preparations, adsorbed onto the mica surface, were not strikingly altered by incubation with either monomeric *or* protofibrillar (predominantly spherical by AFM) α-synuclein. However, the samples pretreated with protofibrillar α-synuclein (WT or A53T) contained several small (diameters of less than 30 nm) ringlike structures (examples in Figure 6). These annular structures were observed *only* upon addition of protofibrillar α-synuclein to brain-derived membrane fractions. In four separate experiments, a total of four annular structures were found after scanning a membrane surface area of 77 μm^2. Analogous experiments involving monomeric WT showed no evidence for any such structures over a scanned area of 80 μm^2. Although the annular structures appear to be derived from protofibrillar α-synuclein, they could also contain other proteins derived from the crude microsomal preparation. However, the fact that the membrane-bound structures closely resemble annular α-synuclein protofibrils that are formed in the absence of membranes (observed by electron microscopy; H. Lashuel et al., unpublished observations) suggests that α-synuclein may be the integral component and that other proteins may not be required for their formation.

Close examination of annular structures formed by membrane-associated WT and A53T protofibrils revealed a "porelike" morphology (diameters of 18, 28, and 23 nm; height above membrane surface of 2−3 nm) (Figure 6). Because of the size and pyramidal shape of the silicon AFM tip used for imaging, it is not possible to accurately determine the shape or the diameter (less than 6 nm) of the putative internal "channel" of these annular structures. However, if these structures are responsible for the in vitro permeabilization activity of α-synuclein protofibrils (*22*), then pore channels of this approximate size could be imagined to allow passage of molecules of less than 2.5 nm in diameter, as is the case for the α-synuclein protofibril (*26*). The annular structures appeared to contain spherical protofibrils as subunits. In one A53T image, a crescent structure was observed (Figure 6C).

DISCUSSION

Formation of annular protofibrils and formation of fibrils both appear to require initial formation of a spherical, β-sheet rich, α-synuclein protofibril. However, the subsequent assembly processes seem to require different conditions. In fact, annular protofibrils are not typically observed in vitro once spherical protofibrils have disappeared and α-synuclein [or β-amyloid peptide (*34*)] is converted to fibrils. Under conditions of "molecular crowding" (*35*), annular protofibrils and fibrils have been observed to coexist, raising the possibility that the former could be more stable under cytoplasmic conditions. We favor a scenario in which the annular protofibrils themselves are not on the *direct* monomer-to-fibril pathway (Figure 7), but must "reopen" to be converted to fibrils. This conversion could involve elongation and annealing of linear chainlike protofibrils (*23*) and/or could involve formation of helices (H. Lashuel et al., manuscript submitted for publication). It is important to note that multiple pathways to the stable fibril may be operative.

The membrane-bound annular protofibrils resemble, in morphology and dimension, β-sheet rich, membrane-spanning pores that are formed by protein toxins (designated β-PFTs, β-sheet pore-forming toxins) (*36*). The β-PFTs include α-hemolysin (*37*), perfringolysin (*38*), and anthrax protective antigen (*39*). Some of these pores share additional features with the α-synuclein annular protofibrils, for example, heterogeneous diameters (*40*), partially formed rings (crescents) (*41*), and a predominance of β-sheet structure in the membrane-bound state (*37*−*39*). It is important to emphasize that the β-PFTs, in contrast to the α-synuclein protofibril, have been optimized by evolution to be selectively cytotoxic. In contrast, the toxic form of α-synuclein is unlikely to have experienced any positive or negative evolutionary pressure. Therefore, the α-synuclein annular protofibril is less stable and more heterogeneous than a typical β-PFT. Its toxicity may be an accident of Nature, a consequence of the fact that protofibrils are intermediates in the pathway to stable and potentially inert amyloid fibrils (*15*, *42*). Whereas a typical β-PFT has been optimized to permeabilize a specific membrane, the toxicity of the annular protofibril may be directed at multiple targets. Inappropriate permeabilization of membranes associated with mitochondria (*43*), dopamine vesicles (*44*), or other organelles could trigger cell death.

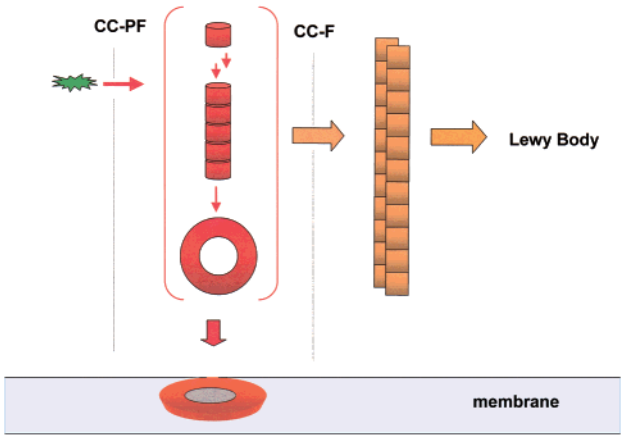

FIGURE 7: Model for the conversion of natively unfolded α-synuclein to spherical and annular protofibrils and fibrils. The initial oligomerization of α-synuclein (green sunburst) to spherical protofibrils (PFs, red cylinders) involves *β*-sheet formation (*22*). Chainlike and annular protofibrils can be produced from the initial spherical species. Some or all of these species may be converted into fibrils, the stable, and possibly inert, component of Lewy bodies. If the critical concentration for PF formation (CC-PF) is lower than the critical concentration for fibril formation (CC-F), as suggested by the work reported here, there would be concentration ranges in which PFs would be populated but fibrils could not form (CC-PF < [α-synuclein] < CC-F). In contrast, if both CC-PF and CC-F were exceeded, PFs would be rapidly consumed and not easily observable. Interestingly, Lewy bodies seem to characterize the surviving neurons in the PD *substantia nigra*, suggesting that cells in which the PF-to-fibril rate is very fast may be less susceptible to death (*54*). It is important to emphasize that the concentrations of the incubations presented here do not directly correspond to intracellular concentrations, since molecular crowding significantly accelerates oligomerization (*35*, *55*).

Membrane permeabilization by protofibrillar intermediates could explain the putative toxicity of other fibrillar proteins that have been implicated in cell death, for example, A*β* in Alzheimer's disease (*45*) and IAPP in type II diabetes (*46*). The in vitro cytotoxicity of these two proteins does not appear to derive from their fibrillar forms (*47*), but rather from a nonfibrillar, oligomeric species whose formation is *linked* to fibrillization (*47*−*49*). Porelike activity has been ascribed to both A*β* (*50*, *51*) and IAPP (*52*). Congo red, which inhibits fibrillization of IAPP, also inhibits formation of the IAPP "channel" (*46*). Finally, membrane-associated, porelike structures comprising A*β* have been observed by AFM (*53*).

If α-synuclein annular protofibrils are the pathogenic species in PD, then inhibition of their formation should be an effective therapeutic strategy (*5*). However, since protofibril annulation and protofibril chain elongation are likely to involve the same *β*-sheet-extending interaction, it is difficult to conceive of a druglike molecule that could answer the question of whether the chain protofibril, the fibril, or the annular protofibril is pathogenic. To address this issue, we are searching for unnatural sequence variants of α-synuclein that optimize annulus formation. Identification of such a variant of α-synuclein could allow production of transgenic animal models in which pathogenesis is very rapid but the "toxic dose" of the transgene is very low and fibrils and/or Lewy bodies are never observed. To test the more specific proposals that α-synucelein annular protofibrils act as pores in vitro and/or in vivo, and that pore formation initiates a pathogenic cascade, we are searching for small molecule inhibitors of in vitro permeabilization, which will then be evaluated in the Parkinsonian mice and/or *Drosophila*.

ACKNOWLEDGMENT

We thank Hilal Lashuel and Mike Volles for their insightful comments regarding the manuscript and Hilal Lashuel for providing the α-synuclein samples used to generate Figure 1.

REFERENCES

1. Rochet, J. C., and Lansbury, P. T. (2000) *Curr. Opin. Struct. Biol. 10*, 60−68.
2. Clayton, D. F., and George, J. M. (1998) *Trends Neurosci. 21*, 249−254.
3. Dunnett, S. B., and Bjorklund, A. (1999) *Nature 399*, A32−A39.
4. Youdim, M. B., and Riederer, P. (1997) *Sci. Am. 276*, 52−59.
5. Goldberg, M. S., and Lansbury, P. T. (2000) *Nat. Cell Biol. 2*, E115−E119.
6. Baba, M., Nakajo, S., Tu, P. H., Tomita, T., Nakaya, K., Lee, V. M., Trojanowski, J. Q., and Iwatsubo, T. (1998) *Am. J. Pathol. 152*, 879−884.
7. Spillantini, M. G., Crowther, R. A., Jakes, R., Hasegawa, M., and Goedert, M. (1998) *Proc. Natl. Acad. Sci. U.S.A. 95*, 6469−6473.
8. Polymeropoulos, M. H., Lavedan, C., Leroy, E., Ide, S. E., Dehejia, A., Dutra, A., Pike, B., Root, H., Rubenstein, J., Boyer, R., Stenroos, E. S., Chandrasekharappa, S., Athanassiadou, A., Papapetropoulos, T., Johnson, W. G., Lazzarini, A. M., Duvoisin, R. C., Di Iorio, G., Golbe, L. I., and Nussbaum, R. L. (1997) *Science 276*, 2045−2047.
9. Nussbaum, R. L., and Polymeropoulos, M. H. (1997) *Hum. Mol. Genet. 6*, 1687−1691.
10. Kruger, R., Kuhn, W., Muller, T., Woitalla, D., Graeber, M., Kosel, S., Przuntek, H., Epplen, J. T., Schols, L., and Riess, O. (1998) *Nat. Genet. 18*, 106−108.
11. Feany, M. B., and Bender, W. W. (2000) *Nature 404*, 394−398.
12. Auluck, P. K., Chan, H. Y. E., Trojanowski, J. Q., Lee, V. M.-Y., and Bonini, N. M. (2001) *Science 295*, 865−868.
13. Masliah, E., Rockenstein, E., Veinbergs, I., Mallory, M., Hashimoto, M., Takeda, A., Sagara, Y., Sisk, A., and Mucke, L. (2000) *Science 287*, 1265−1269.
14. Rochet, J. C., Conway, K. A., and Lansbury, P. T. (2000) *Biochemistry 39*, 10619−10626.
15. Lansbury, P. T. (1999) *Proc. Natl. Acad. Sci. U.S.A. 96*, 3342−3344.
16. Hashimoto, M., Rockenstein, E., Mante, M., Mallory, M., and Masliah, E. (2001) *Neuron 32*, 213−223.
17. Conway, K. A., Lee, S. J., Rochet, J. C., Ding, T. T., Williamson, R. E., and Lansbury, P. T. (2000) *Proc. Natl. Acad. Sci. U.S.A. 97*, 571−576.
18. Conway, K. A., Rochet, J. C., Bieganski, R. M., and Lansbury, P. T. (2001) *Science 294*, 1346−1349.
19. Weinreb, P. H., Zhen, W., Poon, A. W., Conway, K. A., and Lansbury, P. T., Jr. (1996) *Biochemistry 35*, 13709−13715.
20. Conway, K. A., Harper, J. D., and Lansbury, P. T. (1998) *Nat. Med. 4*, 1318−1320.
21. Eliezer, D., Kutluay, E., Bussell, R., and Browne, G. (2001) *J. Mol. Biol. 307*, 1061−1073.
22. Volles, M. J., Lee, S. J., Rochet, J. C., Shtilerman, M. D., Ding, T. T., Kessler, J. C., and Lansbury, P. T., Jr. (2001) *Biochemistry 40*, 7812−7819.
23. Harper, J. D., Wong, S. S., Lieber, C. M., and Lansbury, P. T. (1997) *Chem. Biol. 4*, 119−125.
24. Walsh, D. M., Lomakin, A., Benedek, G. B., Condron, M. M., and Teplow, D. B. (1997) *J. Biol. Chem. 272*, 22364−22372.
25. Li, J., Uversky, V. N., and Fink, A. L. (2001) *Biochemistry 40*, 11604−11613.
26. Volles, M. J., and Lansbury, P. T., Jr. (2002) *Biochemistry 4*, 4595−4602.
27. Conway, K. A., Harper, J. D., and Lansbury, P. T. (2000) *Biochemistry 39*, 2552−2563.
28. Sims, N. R. (1990) *J. Neurochem. 55*, 698−707.
29. Brown, D. A., and Rose, J. K. (1992) *Cell 68*, 533−544.
30. Lee, S. J., Liyanage, U., Bickel, P. E., Xia, W. M., Lansbury, P. T., and Kosik, K. S. (1998) *Nat. Med. 4*, 730−734.

31. LeVine, H. (1997) *Arch. Biochem. Biophys. 342*, 306−316.
32. Saeed, S. M., and Fine, G. (1967) *Am. J. Clin. Pathol. 47*, 588−593.
33. Binnig, G., Quate, C. F., and Gerber, C. (1986) *Phys. Rev. Lett. 56*, 930−934.
34. Harper, J. D., Wong, S. S., Lieber, C. M., and Lansbury, P. T. (1999) *Biochemistry 38*, 8972−8980.
35. Shtilerman, M. D., Ding, T. T., and Lansbury, P. T., Jr. (2002) *Biochemistry 41*, 3855−3860.
36. Heuck, A. P., Tweten, R. K., and Johnson, A. E. (2001) *Biochemistry 40*, 9065−9073.
37. Song, L. Z., Hobaugh, M. R., Shustak, C., Cheley, S., Bayley, H., and Gouaux, J. E. (1996) *Science 274*, 1859−1866.
38. Hotze, E. M., Heuck, A. P., Czajkowsky, D. M., Shao, Z., Johnson, A. E., and Tweten, R. K. (2002) *J. Biol. Chem. 277*, 11597−11605.
39. Benson, E. L., Huynh, P. D., Finkelstein, A., and Collier, R. J. (1998) *Biochemistry 37*, 3941−3948.
40. Malinski, J. A., and Nelsestuen, G. L. (1989) *Biochemistry 28*, 61−70.
41. Czajkowsky, D. M., Sheng, S. T., and Shao, Z. F. (1998) *J. Mol. Biol. 276*, 325−330.
42. Chiti, F., Webster, P., Taddei, N., Clark, A., Stefani, M., Ramponi, G., and Dobson, C. M. (1999) *Proc. Natl. Acad. Sci. U.S.A. 96*, 3590−3594.
43. Hirakura, Y., Yiu, W. W., Yamamoto, A., and Kagan, B. L. (2000) *Amyloid 7*, 194−199.
44. Miller, G. W., Gainetdinov, R. R., Levey, A. I., and Caron, M. G. (1999) *Trends Pharm. Sci. 20*, 424−429.
45. Kawahara, M., and Kuroda, Y. (2000) *Brain Res. Bull. 53*, 389−397.
46. Mirzabekov, T. A., Lin, M. C., and Kagan, B. L. (1996) *J. Biol. Chem. 271*, 1988−1992.
47. Lorenzo, A., Razzaboni, B., Weir, G. C., and Yankner, B. A. (1994) *Nature 368*, 756−760.
48. Hartley, D. M., Walsh, D. M., Ye, C. P. P., Diehl, T., Vasquez, S., Vassilev, P. M., Teplow, D. B., and Selkoe, D. J. (1999) *J. Neurosci. 19*, 8876−8884.
49. Lambert, M. P., Barlow, A. K., Chromy, B. A., Edwards, C., Freed, R., Liosatos, M., Morgan, T. E., Rozovsky, I., Trommer, B., Viola, K. L., Wals, P., Zhang, C., Finch, C. E., Krafft, G. A., and Klein, W. L. (1998) *Proc. Natl. Acad. Sci. U.S.A. 95*, 6448−6453.
50. Janson, J., Ashley, R. H., Harrison, D., McIntyre, S., and Butler, P. C. (1999) *Diabetes 48*, 491−498.
51. Arispe, N., Pollard, H. B., and Rojas, E. (1994) *Mol. Cell. Biochem. 140*, 119−125.
52. Kawahara, M., Kuroda, Y., Arispe, N., and Rojas, E. (2000) *J. Biol. Chem. 275*, 14077−14083.
53. Lin, H., Bhatia, R., and Lal, R. (2001) *FASEB J. 15*, 2433−2444.
54. Tompkins, M. M., and Hill, W. D. (1997) *Brain Res. 775*, 24−29.
55. Minton, A. P. (2000) *Curr. Opin. Struct. Biol. 10*, 34−39.

BI020139H